

Report TW 93

Permeability of plastic disperse systems

by

E.M. de Jager, M.van den Tempel and P. de Bruyne

Permeability of plastic disperse systems

E.M. de Jager^{*}, M.van den Tempel^{**} and P. de Bruyne^{**}

Summary

A theory is presented for the subsidence of plastic disperse systems in unilateral compression. These systems consist of a compressible solid matrix the pores of which are filled with liquid.

Formulae are given for the strain of the solid matrix as a function of position and time and for the rate of subsidence as a function of time.

The theory provides a method for the determination of the average particle size and the compression modulus of a solid network embedded in a liquid. It is successfully applied to results of measurements on several dispersions.

1. Introduction

The measurement of the amount of liquid which flows through a porous solid material under the influence of a hydrostatic pressure constitutes a well known method for the determination of the internal surface area of the solid [1].

In its most simple form, the theory of permeametry assumes that the volume occupied by the liquid per unit volume of the aggregate is independent of the state of stress in the aggregate, i.e. the porosity remains constant during a measurement. This theory can only be used when the solid matrix is unaffected by the forces exerted on a sample of the aggregate during a measurement. It has been applied successfully to the calculation of the effect of seepage of water through ideal sands [2,3].

However, in many disperse systems the three-dimensional network of solid particles is not strong enough to support the stresses required to obtain an appreciable liquid flow. Examples of such systems are filter cakes, clay-type soils and plastic fats. In this case the aggregates are compressible and the porosity depends on the state of stress in the aggregate. In classical soil mechanics [3] it is assumed that the changes

* Mathematical Centre, Amsterdam (Netherlands)

** Unilever Research Laboratory, Vlaardingen (Netherlands)

in the porosity are so small that the coefficients of permeability and compressibility remain constant and uniform in the aggregate. Using this assumption, the consolidation of beds of clay under the influence of unilateral compression is determined by the equation:

$$\frac{\partial h}{\partial t} = \frac{k}{m} \frac{\partial^2 h}{\partial x^2} \quad (1.1)$$

and the appropriate boundary conditions for the excess hydrostatic pressure $h(x,t)$; t denotes the time and x the space coordinate; k is the coefficient of permeability and m is a constant depending on the compressibility of the solid matrix. The solution of (1.1) determines the state of stress in the medium and hence the consolidation of the bed of clay. The mathematical apparatus developed for soil consolidation may be used for many other disperse systems and this is a considerable improvement over the use of the simple permeability theory. Unfortunately, in the case of plastic disperse systems with a low strength of the solid matrix the changes in porosity due to unilateral compression are no longer small and a further extension of the theory is needed.

The theory, presented in this paper, describes the compression of plastic disperse systems. The parameters, appearing in the equations, are related to the structural properties of the material, in particular the compressibility and the surface area of the solid matrix are determined.

2. Description of the plastic disperse system

We consider an aggregate of solid particles forming a three-dimensional solid network the pores of which are filled with liquid.

We investigate the behaviour of this aggregate during compression, while the liquid can escape through a part of the boundary of the aggregate.

In particular we consider a homogeneous plug of the material which is contained in an undeformable cylinder. The cylinder is closed on one side by a filter which allows the free passage of liquid but not of solid. The other side of the cylinder is closed by an impermeable and frictionless plunger or by a column of fluid which can penetrate into the aggregate (see fig.1). The plug is compressed in the first case by applying some

load to the plunger and in the latter case by the weight of the column of fluid.

We determine in this paper the state of stress and the subsidence of the plug, using the following assumptions.

The liquid and the solid are incompressible. The pores in the material are small in comparison with the dimensions of the specimen and they remain filled with liquid during the compression of the plug.

Considering one-dimensional compression the state of stress is the same in every point of every horizontal section through the plug and for every stage of the process; friction at the wall of the cylinder is neglected.

Darcy's law is strictly valid within any infinitely thin horizontal slice of the plug; the coefficient of permeability is a function of position and time.

At the outset of the consolidation process the specimen is in mechanical equilibrium and has a uniform porosity.

The behaviour of the plastic disperse system is completely described by the following five quantities: the velocity \underline{v}_s of the solid particles with respect to the cylinder, the mean velocity \underline{v}_l of the fluid particles with respect to the surrounding solid, the effective normal stress \underline{p} , the excess hydrostatic pressure \underline{h} and the porosity $\underline{\epsilon}$. The porosity $\underline{\epsilon}$ is defined as the fraction of an infinitesimal volume occupied by liquid.

The velocities will be taken positive in downward direction.

Investigating unilateral compression we need only one space coordinate x with $\underline{x}=0$ at the filter (see fig.1). In order to obtain fixed boundaries the above mentioned quantities will be expressed as functions of the Lagrangian variable \underline{a} and the time \underline{t} ; \underline{a} is the position of a solid particle at time $\underline{t}=0$. The use of the independent variables \underline{a} and \underline{t} is illustrated in figure 2, where the position $\underline{x}(\underline{a},\underline{t})$ of a solid particle is sketched as a function of \underline{a} and \underline{t} . At time $\underline{t}=0$ $\underline{x}=\underline{x}(\underline{a},0)=\underline{a}$, which is represented by the straight line OA ; $A'A$ is the height of the plug at time $\underline{t}=0$. After some time \underline{t}_1 this height has been reduced to $H'H$ and the graph of $\underline{x}=\underline{x}(\underline{a},\underline{t}_1)$ is given by the curve BH . The tangent to the curve AH yields the velocity of the upper surface of the plug, e.g. the velocity of the plunger after some load has been applied to it.

To determine the quantities $\underline{v}_1, \underline{v}_s, \underline{p}, \underline{h}$ and $\underline{\epsilon}$ we need five equations and appropriate boundary conditions connecting them.

3. The differential equations describing the behaviour of the aggregate during consolidation

a The equation of continuity for the liquid

The net liquid flow during a time interval Δt from a thin horizontal slice of the aggregate with boundaries $\underline{x}=\underline{x}_1$ and $\underline{x}=\underline{x}_2$ equals the change in liquid content of the slice during the time interval Δt . Expressing this mathematically we obtain:

$$\left\{ \epsilon(a_1, t) v_1(a_1, t) - \epsilon(a_2, t) v_1(a_2, t) \right\} \Delta t = \left[\left\{ x_1 - v_s(a_1, t) \Delta t \right\} - \left\{ x_2 - v_s(a_2, t) \Delta t \right\} \right] \epsilon\left(\frac{a_1+a_2}{2}, t + \Delta t\right) - (x_1 - x_2) \epsilon\left(\frac{a_1+a_2}{2}, t\right)$$

where \underline{a}_1 and \underline{a}_2 are the positions of the boundaries $\underline{x}=\underline{x}_1$ and $\underline{x}=\underline{x}_2$ at $\underline{t}=0$. Taking on both sides the limit for $(\underline{x}_1 - \underline{x}_2) \rightarrow 0$ and $\Delta(\underline{t}) \rightarrow 0$ we get:

$$\left\{ \frac{\partial}{\partial a} (\epsilon v_1) + \epsilon \frac{\partial v_s}{\partial a} \right\} \frac{\partial a}{\partial x} = \frac{\partial \epsilon}{\partial t} \quad (3.1)$$

b The equation of continuity for the solid

Since the amount of solid within a horizontal slice with boundaries $\underline{x}=\underline{x}_1(\underline{a}_1, \underline{t})$ and $\underline{x}=\underline{x}_2(\underline{a}_2, \underline{t})$ is independent of time, we have the relation:

$$\frac{\partial x}{\partial a} = \frac{1 - \epsilon_0}{1 - \epsilon} \quad (3.2)$$

where ϵ_0 is the uniform porosity at $\underline{t}=0$.

Differentiating this relation with respect to \underline{t} yields:

$$\frac{\partial v_s}{\partial a} = - \frac{\partial}{\partial t} \left(\frac{1 - \epsilon_0}{1 - \epsilon} \right)$$

or

$$(1 - \epsilon) \frac{\partial v_s}{\partial a} \frac{\partial a}{\partial x} = - \frac{\partial \epsilon}{\partial t} \quad (3.3)$$

Adding now the eqs. (3.1) and (3.3) we obtain instead of (3.1) the simpler formula:

$$\frac{\partial}{\partial a} (v_s + \varepsilon v_l) = 0 \quad (3.4)$$

Introducing the strain $\xi(a, t)$ of the solid matrix, defined by:

$$\xi(a, t) = 1 - \frac{\partial x}{\partial a} \quad (3.5)$$

we get by aid of (3.2)

$$\xi(a, t) = \frac{\varepsilon_0 - \varepsilon}{1 - \varepsilon} \quad (3.6)$$

Differentiating (3.5) with respect to the time yields the well known relation of the theory of elasticity:

$$\frac{\partial v_s}{\partial a} = \frac{\partial \xi}{\partial t} \quad (3.7)$$

c The equation of motion for the liquid

The equation of motion for the liquid is given by the well known formula of Darcy [4] :

$$v_l = \frac{F(\varepsilon)}{\mu} \frac{\partial h}{\partial x} \quad (3.8)$$

where μ denotes the viscosity of the liquid and $F(\varepsilon)$ the permeability of the medium. The dependency of the permeability on the porosity ε is assumed to be that of the Kozeny-Carman relation [5,6] :

$$F(\varepsilon) = \frac{1}{c S^2} \left(\frac{\varepsilon}{1 - \varepsilon} \right)^2 \quad (3.9)$$

where S is the surface area of the solid particles (cm^2 per cm^3 of solid) and c a geometrical constant having the value 5.0 [7,8].

Transforming to the Lagrangian variable a and using (3.2) equation (3.8) becomes:

$$\frac{1 - \varepsilon_0}{1 - \varepsilon} v_l = \frac{F(\varepsilon)}{\mu} \frac{\partial h}{\partial a} \quad (3.10)$$

d The equation for the equilibrium of forces

When a pressure P depending eventually on t , is applied to the plug, this pressure P is carried partly by the solid network, yielding an effective normal stress $p(a, t)$ and partly by the pore liquid, giving rise to an

excess hydrostatic pressure $\underline{h}(\underline{a}, \underline{t})$.

Neglecting inertia we may write:

$$p(\underline{a}, \underline{t}) + h(\underline{a}, \underline{t}) = P(\underline{t}) \quad (3.11)$$

or

$$\frac{\partial p}{\partial \underline{a}} + \frac{\partial h}{\partial \underline{a}} = 0 \quad (3.12)$$

e The stress-strain relation for the network

The effective normal stress $\underline{p}(\underline{a}, \underline{t})$ on the solid matrix causes a strain $\underline{\xi}(\underline{a}, \underline{t})$; the relation between them, the stress-strain relation, is still unknown. Assuming that the solid matrix is purely elastic, the stress-strain relation does not contain the time and we may write:

$$p = p(\underline{\xi}) \quad (3.13)$$

This means that any increase in effective normal stress results in an immediate compression of the matrix without time lag and to such an extent, that the compressed matrix can support the increased effective stress. without any further change. The compression of the matrix is actually a slow process and so the effective normal stress varies also slowly; this is not due to a property of the matrix itself but to the liquid in the pores, which must be partially removed before the compression is at its final value.

In the following we shall postulate a stress-strain relation in such a way that the mathematical analysis will be simplified considerably; the experimental verification of this postulated stress-strain is given in sections 11 and 12.

f The differential equation for the strain $\underline{\xi}(\underline{a}, \underline{t})$.

Eliminating $\underline{h}(\underline{a}, \underline{t})$ from the eqs. (3.10) and (3.12) we obtain:

$$v_1(\underline{a}, \underline{t}) = - \frac{F(\underline{\xi})}{\mu} \frac{1-\underline{\xi}}{1-\underline{\xi}_0} \frac{\partial p}{\partial \underline{a}}$$

and hence by aid of (3.4)

$$\frac{\partial v_s}{\partial \underline{a}} = \frac{\partial}{\partial \underline{a}} \left\{ \underline{\xi} \frac{1-\underline{\xi}}{1-\underline{\xi}_0} \frac{F(\underline{\xi})}{\mu} \frac{\partial p}{\partial \underline{a}} \right\}.$$

Using finally (3.7), (3.13) and (3.6) the differential equation for the strain $\xi(a, t)$ becomes:

$$\frac{\partial \xi}{\partial t} = \frac{\partial}{\partial a} \left[\frac{F(\xi)}{\mu} \frac{\xi_o^{-\xi}}{(1-\xi)^2} \frac{dp}{d\xi} \frac{\partial \xi}{\partial a} \right] \quad (3.14)$$

with

$$F(\xi) = \frac{1}{5 S^2} \left(\frac{\xi_o^{-\xi}}{1-\xi_o} \right)^2 \quad (3.15)$$

Multiplying both sides of (3.14) with $\frac{dp}{d\xi}$ yields the differential equation for the effective normal pressure $p(a, t) = p(\xi)$, viz:

$$\frac{\partial p}{\partial t} = \frac{dp}{d\xi} \frac{\partial}{\partial a} \left[\frac{F(\xi)}{\mu} \frac{\xi_o^{-\xi}}{(1-\xi)^2} \frac{\partial p}{\partial a} \right] \quad (3.16)$$

By aid of (3.11) we obtain the differential equation for the excess hydrostatic pressure $h(a, t)$:

$$\frac{\partial h}{\partial t} = \frac{dp}{d\xi} \frac{\partial}{\partial a} \left[\frac{F(\xi)}{\mu} \frac{\xi_o^{-\xi}}{(1-\xi)^2} \frac{\partial h}{\partial a} \right] \quad (3.17)$$

This equation is the generalization of the differential equation (1.1), which is usually taken as the starting point for the determination of the consolidation of beds of clay in classical soil mechanics.

The differential equations (3.14), (3.16) and (3.17) are complicated non-linear differential equations containing the still completely unknown factor $\frac{dp}{d\xi}$.

The solution of the problem is simplified considerably if one of these equations can be linearized.

The linearization of the equations (3.16) and (3.17) would involve that we have to take $\frac{F(\xi)}{\mu} \frac{\xi_o^{-\xi}}{(1-\xi)^2}$ and $\frac{dp}{d\xi}$ as constants, while the linearization of equation (3.14) involves the assumption that the product of $\frac{F(\xi)}{\mu} \frac{\xi_o^{-\xi}}{(1-\xi)^2}$ and $\frac{dp}{d\xi}$ may be taken as a constant.

Since the latter linearization leaves us more freedom to approximate the physical reality, we focus our attention to the linearization of the differential equation for the strain.

We assume now that under certain conditions of the experiment it is allowed to put

$$F(\xi) \frac{\varepsilon_0 - \xi}{(1-\xi)^2} \frac{dp}{d\xi} = \text{constant} = A \quad (3.18)$$

and the differential equation for the strain becomes:

$$\frac{\partial \xi}{\partial t} = A' \frac{\partial^2 \xi}{\partial a^2} \quad (3.19)$$

with $A' = \frac{A}{\mu}$ (3.20)

The validity of this linearization procedure and the conditions to which the material has to be submitted in order that (3.18) holds are investigated in sections 11, 12 and 13.

4. The stress-strain relation

By aid of (3.15) we may write instead of (3.18):

$$\frac{dp}{d\xi} = A \cdot 5 S^2 \cdot (1-\xi_0)^2 \frac{(1-\xi)^2}{(\varepsilon_0 - \xi)^3} \quad (4.1)$$

where \underline{A} is a certain constant for the material considered.

Using (3.6) the stress-strain relation can be expressed as a function of the porosity ε as follows:

$$\frac{dp}{d\xi} = A \cdot 5 S^2 \cdot \frac{(1-\varepsilon_0)(1-\varepsilon)}{\varepsilon^3} \quad (4.2)$$

Equation 4.2 shows that the resistance of the solid matrix against compression increases rapidly with increasing solid content $(1-\varepsilon)$ and with decreasing particle size.

It depends further on a property of the network connected with the symbol \underline{A} which has the dimension of a force. The quantity \underline{A} describes the influence of the strength of the bonds between neighbouring particles in the network. Application of the theory developed in this paper is restricted to cases where \underline{A} is a constant and this means, that compression of the network should not result in irreversible breaking of the bonds between the particles.

It will be shown in sect. 8-10 that it is possible to carry out experiments in such a way that the results can be described with a constant value of

A. Integrating eq. (4.1) with the condition $p(0)=0$ yields after some elementary calculations the following expression for $p(\xi)$ as function of ξ :

$$p(\xi) = A \cdot 5 \cdot S^2 \cdot (1 - \xi_0)^2 Q(\xi_0, \xi) \quad (4.3)$$

with

$$Q(\xi_0, \xi) = \frac{1 - \xi_0}{2 \xi_0^2} \xi \frac{2 \xi_0 (1 + \xi_0) - (1 + 3 \xi_0) \xi}{(\xi_0 - \xi)^2} + \log \frac{\xi_0}{\xi_0 - \xi} \quad (4.4)$$

A graph of the function $Q(\xi_0, \xi)$ for various values of ξ_0 is given in figure 3.

5. Boundary conditions

In order to solve the differential equation (3.19) we have now to specify the boundary conditions to be satisfied by $\xi(a, t)$. We consider for the time being the case that the plug is compressed due to a loaded impermeable frictionless plunger.

At $t=0$ the porosity has not yet changed and we have:

$$\xi(a, t) \equiv 0 \quad \text{for } t=0 \quad \text{and } 0 < a \leq b_0 \quad (5.1)$$

where b_0 is the height of the plug at $t=0$.

During the compression of the plug the excess hydrostatic pressure in the layer adjoining the filter equals always zero and hence the effective normal stress $p(a, t) = p(\xi)$ equals the applied load P for $a=0$ and $0 < t < \infty$ (see equ. 3.11). Consequently, we obtain for the strain $\xi(a, t)$ the condition:

$$\xi(a, t) \equiv \xi^* \quad \text{for } a=0 \quad \text{and } 0 < t < \infty \quad (5.2)$$

where ξ^* is determined by formula (4.3) with

$$p(\xi^*) = P \quad (5.3)$$

Since we assume that the pores of the aggregate remain filled with liquid during the compression, we have also the condition

$$v_1(b_0, t) \equiv 0 \quad \text{for } 0 < t < \infty$$

It follows from eqs. (3.10) and (3.11) that $\frac{\partial p}{\partial a}(b_0, t)$ equals zero for

all values of \underline{t} . Since $\frac{\partial p}{\partial \underline{a}} = \frac{\partial p}{\partial \xi} \frac{\partial \xi}{\partial \underline{a}}$ and $\frac{dp}{d\xi}$ is not identically zero for $\underline{a}=\underline{b}_0$ (see (4.2)), we get finally at the upper boundary of the specimen the condition:

$$\frac{\partial \xi}{\partial \underline{a}} \equiv 0 \quad \text{for } \underline{a}=\underline{b}_0 \text{ and } 0 < t < \infty \quad (5.4)$$

The conditions (5.1), (5.2) and (5.4) suffice to determine uniquely the function $\xi(\underline{a}, \underline{t})$ from the differential equation (3.19).

6. The compression due to a loaded plunger

Using a constant load \underline{P} the equation (3.19) with the conditions (5.1), (5.2) and (5.4) can be solved by means of e.g. the method of Laplace transformation [9]. The result is:

$$\xi(\underline{a}, \underline{t}) = \xi^* - 2 \xi^* \sum_{n=0}^{\infty} \exp \left\{ -A' (n+\frac{1}{2})^2 \pi^2 \frac{t}{b_0} \right\} \frac{\sin \left\{ (n+\frac{1}{2}) \pi \frac{a}{b_0} \right\}}{(n+\frac{1}{2}) \pi} \quad (6.1)$$

where ξ^* is a certain constant defined by (5.3).

This expression converges for all values of \underline{a} and \underline{t} ; however for small values of $\underline{A}'\underline{t}$ the convergence of (6.1) is very slow and therefore it is useful to give also a series expansion which is more suitable than (6.1) for small values of $\underline{A}'\underline{t}$.

Expanding the Laplace transform of $\xi(\underline{a}, \underline{t})$, which is denoted by $\bar{\xi}(\underline{a}, \underline{s})$, into a series which converges for large values of \underline{s} and transforming inversely term by term we obtain the result:

$$\xi(\underline{a}, \underline{t}) = \xi^* \sum_{n=0}^{\infty} \left[(-1)^n \operatorname{erfc} \left(\frac{2n b_0 + a}{2 \sqrt{A' t}} \right) + (-1)^n \operatorname{erfc} \left(\frac{2(n+1) b_0 - a}{2 \sqrt{A' t}} \right) \right] \quad (6.2)$$

with $\operatorname{erfc} a = \frac{2}{\sqrt{\pi}} \int_a^{\infty} e^{-v^2} dv$.

The terms of the asymptotic series (6.2) fall off rapidly for small values of $\underline{A}'\underline{t}$ and therefore this expansion is to be preferred above the expansion (6.1) for small values of $\underline{A}'\underline{t}$.

According to the magnitude of \underline{t} the porosity ξ can now be obtained by aid of (3.6) from (6.1) or (6.2).

Using the differential equations (3.7) and (3.4) one can derive expansions, analogous to (6.1) and (6.2), for the velocity $\underline{v}_s(\underline{a}, \underline{t})$ and the discharge

velocity $\xi(\underline{a}, \underline{t}) \underline{v}_1(\underline{a}, \underline{t})$. The excess hydrostatic pressure can be obtained by aid of the equation of Darcy (3.10) which has to be integrated numerically; from the relation (3.11) follows finally the effective normal stress.

We confine our calculations to the determination of the velocity $\underline{v}_s(\underline{a}, \underline{t})$ of the solid particles. Differentiating (6.1) and (6.2) with respect to \underline{t} and integrating consecutively from zero to some value of \underline{a} , we get the results:

$$\underline{v}_s(\underline{a}, \underline{t}) = + \frac{2 \mathfrak{F}^* A'}{b_o} \sum_{n=0}^{\infty} \exp \left\{ -A' (n+\frac{1}{2})^2 \pi^2 \frac{\underline{t}}{b_o^2} \right\} \left\{ 1 - \cos \left((n+\frac{1}{2}) \pi \frac{\underline{a}}{b_o} \right) \right\} \quad (6.3)$$

and

$$\begin{aligned} \underline{v}_s(\underline{a}, \underline{t}) = \mathfrak{F}^* \sqrt{\frac{A'}{\pi}} \frac{1}{\sqrt{\underline{t}}} & \left[1 + 2 \sum_{n=1}^{\infty} (-1)^n \exp \left(- \frac{n^2 b_o^2}{A' \underline{t}} \right) - \right. \\ & \left. - \sum_{n=0}^{\infty} (-1)^n \exp \left\{ - \frac{(2n b_o + \underline{a})^2}{4 A' \underline{t}} \right\} + \sum_{n=0}^{\infty} (-1)^n \exp \left\{ - \frac{(2(n+1) b_o - \underline{a})^2}{4 A' \underline{t}} \right\} \right] \end{aligned} \quad (6.4)$$

Putting $\underline{a} = b_o$ we obtain the velocity of the plunger as function of \underline{t} ; the results are:

$$\underline{v}(\underline{t}) = + \frac{2 \mathfrak{F}^* A'}{b_o} \sum_{n=0}^{\infty} \exp \left\{ -A' (n+\frac{1}{2})^2 \pi^2 \frac{\underline{t}}{b_o^2} \right\} \quad (6.5)$$

and

$$\underline{v}(\underline{t}) = \mathfrak{F}^* \sqrt{\frac{A'}{\pi}} \frac{1}{\sqrt{\underline{t}}} \left[1 + 2 \sum_{n=1}^{\infty} (-1)^n \exp \left(- \frac{n^2 b_o^2}{A' \underline{t}} \right) \right] \quad (6.6)$$

For small values of $A' \underline{t}$ we use the expansion (6.6) instead of (6.5). Finally we determine the amount $\underline{R}(\underline{t})$ of liquid which has percolated per unit area through the filter during the time \underline{t} . This quantity equals the decrease of the height of the sample at time \underline{t} . Since the latter can easily be determined experimentally, it is worthwhile to give an expression for the height of the plunger at time \underline{t} .

Denoting this quantity by $\underline{b}(\underline{t})$ we may write:

$$\underline{b}(\underline{t}) = b_o - \int_0^{\underline{t}} \underline{v}(\tau) d\tau \quad (6.7)$$

substituting (6.5) into (6.7) we obtain for the decrease of the height of the plunger:

$$R(t) = b_0 - b(t) = \int_0^t v(\tau) d\tau = b_0 \mathcal{J}^* \left[1 - \frac{8}{\pi^2} \sum_{n=0}^{\infty} \frac{\exp \left\{ -A' (n + \frac{1}{2})^2 \pi^2 \frac{t}{b_0^2} \right\}}{(2n+1)^2} \right] \quad (6.8)$$

Hence the degree U of subsidence can be expressed as:

$$U = 100 \left[1 - \frac{8}{\pi^2} \sum_{n=0}^{\infty} \frac{\exp \left\{ -A' (n + \frac{1}{2})^2 \pi^2 \frac{t}{b_0^2} \right\}}{(2n+1)^2} \right] \% \quad (6.9)$$

In order to obtain a series more suitable than (6.8) for small values of $\underline{A't}$ we substitute (6.6) into the formula (6.7). The result is:

$$R(t) = b_0 - b(t) = 2 \mathcal{J}^* \sqrt{\frac{A'}{\pi}} \sqrt{t} + 2 \mathcal{J}^* \sqrt{\frac{A'}{\pi}} \sum_{n=1}^{\infty} (-1)^n \int_0^t \frac{\exp(-\frac{n^2 b_0^2}{A' \tau})}{\sqrt{\tau}} d\tau \quad (6.10)$$

For small values of $\underline{A't}$ we may write approximately:

$$R(t) = b_0 - b(t) \approx 2 \mathcal{J}^* \sqrt{\frac{A'}{\pi}} \sqrt{t} \quad (6.11)$$

and hence $R(t)$ is approximately proportional to \sqrt{t} . This proportionality is known as the square root law of Terzaghi [3]; this law has been generalized by Mc Nabb [10], using a dimensional analysis. However, the formulation of this square root law in the form of equation (6.11) will appear to be very useful for the application of the theory to plastic disperse systems with a solid matrix of low strength.

The case of filtration

During filtration the plug is compressed by a column of liquid placed on top of the specimen, while the liquid of this column can penetrate into the aggregate. The boundary conditions at $\underline{t}=0$ and $\underline{a}=0$ do not differ essentially from those of section 5. However, the condition at $\underline{a}=\underline{b}_0$ changes substantially since the excess hydrostatic pressure at $\underline{a}=\underline{b}_0$ equals the pressure exerted on the plug by the weight of the column of liquid. It follows that during filtration the effective normal stress and hence also the strain \mathcal{E} equals zero for $\underline{a}=\underline{b}_0$. (see eq.3.11). So we obtain instead of the boundary condition

(5.4) the condition:

$$\mathcal{J}(\underline{a}, \underline{t}) \equiv 0 \quad \text{for } \underline{a} = \underline{b}_0 \quad \text{and } 0 \leq t < \infty \quad (7.1)$$

In the same way as in section 6 the strain $\mathcal{J}(\underline{a}, \underline{t})$, the velocities $\underline{v}_s(\underline{a}, \underline{t})$ and $\underline{v}(\underline{t})$ and the subsidence $\underline{b}_0 - \underline{b}(\underline{t})$ can be calculated and the resulting formulae are quite analogous to those of section 6. In particular, the subsidence $\underline{b}_0 - \underline{b}(\underline{t})$ has the same form as equation (6.10), except a slight modification in the second term of the right hand side. Hence we obtain again for small values of $\underline{A}'\underline{t}$ the result:

$$\underline{b}_0 - \underline{b}(\underline{t}) \approx 2 \sqrt{\frac{\underline{A}}{\pi}} \sqrt{\underline{t}} \quad (7.2)$$

8. Experimental verification of the theory

The proposed stress-strain relation for the solid matrix is given by equation (4.2), where \underline{A} is a constant for the material under investigation, and should be independent of the value of \mathcal{E} and of the pressure used. The values of \underline{A} and \underline{S} for a material with given initial porosity are obtained from measurements of the rate of subsidence at two different values of the pressure. If the results of measurements over a large range of pressure values can be described with the same values of \underline{A} and \underline{S} , this proves that \underline{A} is independent of the pressure in that range.

Since the non-uniform variation of the porosity depends strongly on the applied pressure, this result also proves that \underline{A} is independent of the porosity.

A more sensitive check is obtained by performing experiments on materials having the same particles dispersed in different concentrations.

9. Description of the experiment

Most of the experiments were carried out in the instrument of which fig.4 shows an exploded view. The specimen is contained in the cylindrical holder A, which is closed at the bottom by means of one disc of filter paper (B) and a perforated metal disc (C). A capillary is connected to the upper end of A by means of a short piece of plastic tubing (not shown). The metal disc is held in position by the threaded tube F. This tube is connected at E to a vessel containing a constant subatmospheric pressure. The oil-resistant rubber ring D prevents leakage of air between A and F.

The apparatus is assembled after the filter paper has been wetted with a small amount of the liquid present in the porous material. The space A is then filled with the freshly-worked sample, taking care that no inhomogeneities are introduced. The capillary is filled with a liquid which is non-miscible with the liquid present in the porous material; a light oil is used if the sample contains water and water is present in the capillary if the sample contains oil.

The oil-water interface acts as an impermeable and frictionless plunger, since no penetration of the capillary liquid into the sample takes place at the pressure applied. The assembled instrument is submerged in a water bath held at 20.0°C , and 5 min. are allowed to establish temperature equilibrium. The suction line is then opened, and readings of the liquid level in the capillary are taken at frequent intervals.

The crosssectional area of the specimen was in most experiments 100 x the area of the capillary. The change in sample height is then easily found from the capillary readings, and this is plotted against the square-root of time. Fig.5 shows typical examples of the resulting straight lines. (see eq.6.11). The measurement is repeated with a fresh sample of the same material, but using a different value of the pressure.

10. Materials

Dispersions in oil were produced by controlled crystallization of glyceryl tristearate from its hot solution in oil. The solubility of tristearate in oil at room temperature is negligible, and hence the porosity of the sample can be calculated from its composition and the known density values for oil and tristearate.

The surface area of the fat crystals in these materials can be varied between about 3 and $130\text{ m}^2\text{ per cm}^3$ of solid fat, depending only on the nucleation temperature and hence on the rate of cooling when crystallization is initiated. Samples have been made in liquid paraffin oil and in liquid triglyceride oils.

Plastic dispersions containing inorganic powders were made in water or in paraffin oil. The powders consisted of silica or of TiO_2 ; their surface area had been determined by means of nitrogen adsorption measurement at low temperature (B.E.T.-method).

11. Application of the theory

In the theory developed in section 1-8 of this paper, it is considered that the behaviour of a sample in a compression test is completely determined by two independent properties of the material: the internal surface area \underline{S} and the parameter \underline{A} which measures the strength of the links between consecutive particles in the network. Any single experiment results only in a value for a certain combination of these parameters. The values of each of these parameters separately can be obtained from the results of two measurements, on identical samples, using different values of the pressure.

In an experiment of relatively short duration the height of the specimen decreases with time in accordance with

$$\Delta b = 1.128 \mathcal{S}^* \sqrt{A' t} \quad (11.1)$$

In two compression tests, with identical samples and using pressures \underline{P}_1 and \underline{P}_2 , the slopes of the straight lines in a plot of Δb vs. the square root of time are proportional to the values of \mathcal{S}^* in these experiments, since $\underline{A}' = \frac{\underline{A}}{\mu}$ was postulated to be independent of the pressure. Hence the ratio of the values of the strain in the layer adjoining the filter, denoted by \mathcal{S}_1^* respectively \mathcal{S}_2^* , can be measured. A second relation between these strain values is found by applying equations (4.3) and (5.3):

$$\frac{P_1}{P_2} = \frac{Q(\epsilon_o, \mathcal{S}_1^*)}{Q(\epsilon_o, \mathcal{S}_2^*)} \quad (11.2)$$

A graphical method has been used for solving these two equations in the two unknown parameters \mathcal{S}_1^* and \mathcal{S}_2^* . Graphs were constructed giving \mathcal{S}_1^* as a function of the ratio $\mathcal{S}_1^*/\mathcal{S}_2^*$ for a given value of P_1/P_2 and for various values of ϵ_o . An example of such a graph is shown in fig.6. If the value of \mathcal{S}_1^* has been obtained from this graph and the results of two measurements, the value of \underline{A}' is found from equation (11.1) and consecutively the value of \underline{S} from equations (3.20) and (4.3).

12. Results

The effects of pressure and of initial porosity on the rate of subsidence of plastic fats are recorded in fig.7 and 8. Here, the slope of the straight line obtained from a plot of the plug height vs. the square root of time has been plotted against the pressure used in the consolidation test.

In each case the sample having the higher porosity value was obtained from the sample containing the highest concentration of tristearate, by dilution with oil. This was performed by mixing the plastic fat with the required amount of oil and kneading the mixture with a spatula on a glass plate until it appeared homogeneous. It is assumed that the size of the extremely small fat crystals is not appreciably affected by this treatment.

Fig.9 relates to a material containing powdered quartz in groundnut oil. The surface area of this powder, measured by means of the B.E.T.-method, was 4 m^2 per cm^3 of quartz. The slightly lower value found from permeability measurements may be explained by the irregular surface of these particles, of which only an envelope is measured by the permeability method. The B.E.T.-surface of the rutile powder shown in fig.10 was $2.76 \times 10^6 \text{ cm}^{-1}$.

13. Discussion

The results presented in figs. 7 - 9 show that the stress-strain relation of the solid network is given by equation (4.2), in which A is independent of the pressure and the porosity within the experimental error. The compressibility of the network of solid particles is determined by the number of links between the particles, and the strength of these links. In a freshly worked sample, the number of interparticle links in the network is completely determined by the particle concentration, and its effect on the compressibility of the network is accounted for in the factors containing S and ε in equation (4.2). It follows that the parameter A must represent the strength of the interparticle links.

The stress-strain relation (4.2) can only be valid if both the structure of the network and the properties of the interparticle links are unaffected by the compression resulting from a measurement. In the undisturbed, freshly worked material a network is rapidly formed by flocculation of the dispersed particles, and this is the network of which the compressibility depends on \underline{S} and $\underline{\epsilon}$ as shown in equation (4.2). Unilateral compression of this network must result in structural changes, i.e. both the number of interparticle links and their average strength will be different from those in the network formed by flocculation only. This means that strong local compression at rather high pressures can no longer be described by equation (4.2) with the value of \underline{A} for the undisturbed network. It was found experimentally that the rate of subsidence tended to be higher than predicted at high pressure values (cf. fig.9). In the type of materials investigated, constant values of \underline{A} were generally found in the range of pressure values which resulted in a rate of subsidence between about 10^{-4} and 12×10^{-4} cm sec.^{-1/2}.

Application of the theory developed in this paper to filtration problems would require \underline{A} to be independent of the porosity in a very large range of porosity values. It has been found that the behaviour of the system can not be described satisfactorily with a constant value of \underline{A} if large variations in the porosity can occur. This is attributed to differences in the network structure produced in dilute and in concentrated suspension.

The compression modulus of the undisturbed network is obtained by inserting $\underline{\epsilon} = \underline{\epsilon}_0$ in equation (4.2). Values for the samples described in figs. 7 and 9 are between 10^4 and 4×10^5 dynes cm⁻², which is about 100 x lower than the values of the shear modulus of the solid network in materials of this type [11]. This can be understood by considering that the shear modulus depends on the force required for breaking of links between particles, whereas in compression only bending of chains of particles is required and no links need be broken.

Finally, it should be noticed that the stress-strain relation (4.1) of the solid network in unilateral compression predicts large deviations from linear (Hookean) behaviour already at small deformations.

Actually, in the separate determination of the compression modulus of the network and of the internal surface area, use is made of the non-linearity of the rheological behaviour in compression. The behaviour in shear of plastic-disperse systems had already been found to deviate from linearity [11], and also in that case accurate measurements of the deviation from linear behaviour could be used in relating the internal structure with the mechanical properties of these materials.

Literature

1. Orr, C. Fine Particle Measurement, New York 1959,
Dallavalle, J.M. Chapter 6.
2. Muskat, M. The Flow of Homogeneous Fluids through Porous Media. J.W. Edwards, Ann Arbor, Michigan, 1946
Chs IV and V
3. Terzaghi, K. Theoretical Soil Mechanics, sec.ed. Wiley,
New York, Chs XII and XIII
4. Darcy, H. Les Fontaines Publiques de la Ville de
Dyon (1856)
5. Carman, P.C. Trans. Inst.Chem.Engrs 15, 150 (1937)
6. Debye, P. J. Appl.Physics, 30, 843, (1959)
Cleland, R.L.
7. Dodd, C.G. et al. J. Phys. Chem., 55, 684 (1951)
8. Johansen, R.T. et al. J. Phys. Chem., 57, 40 (1953)
9. Churchill, R.V. Modern Operational Mathematics in Engineering,
Mc Graw-Hill, New York, 1944
10. Mc Nabb, A. A Mathematical Treatment of One-dimensional
Soil Consolidation, Quart.Appl.Math. 17, 337
(1960)
11. van den Tempel, M. J. Colloid Sci. 16, 284 (1961)

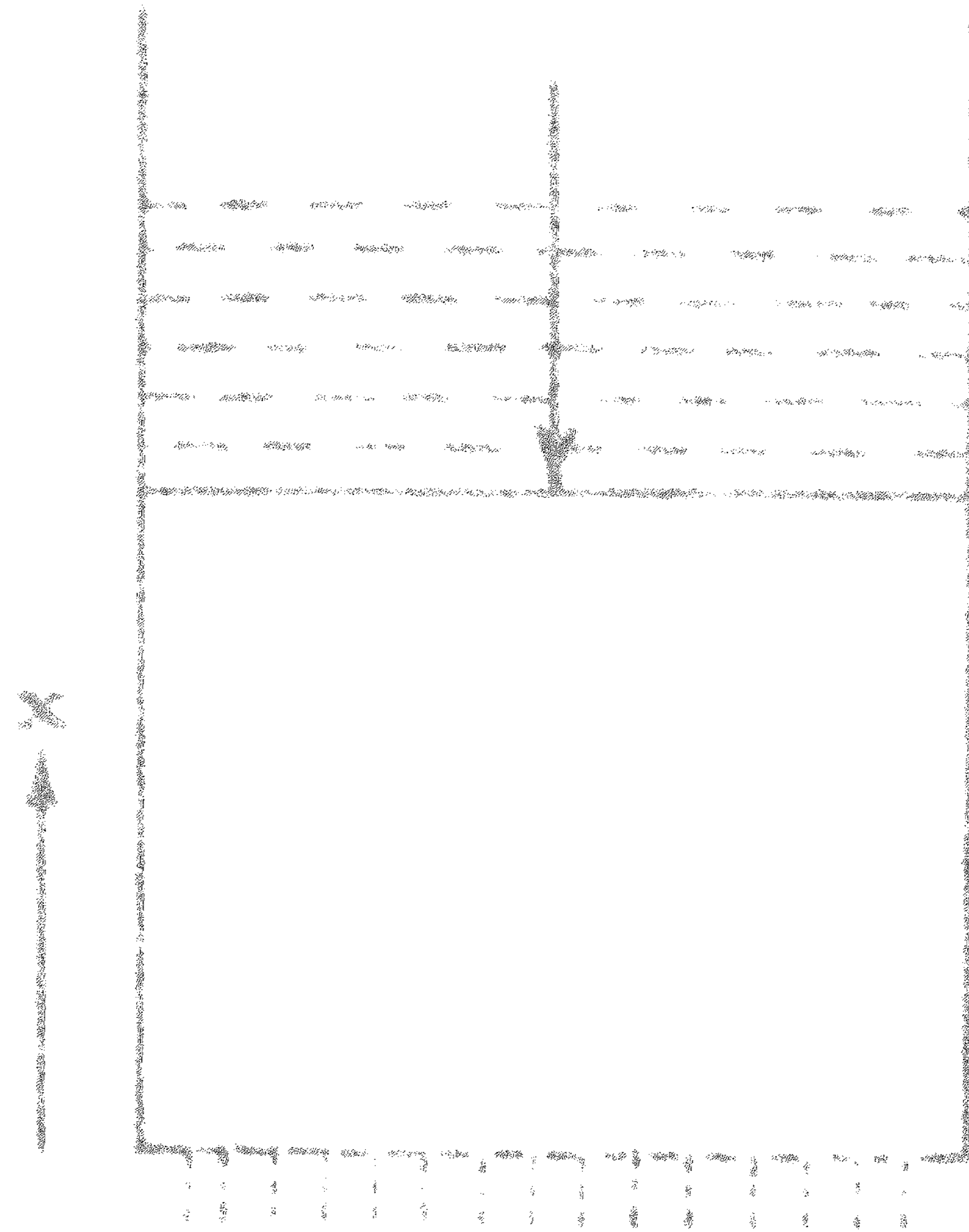


fig.1

Schematic view of plug under compression

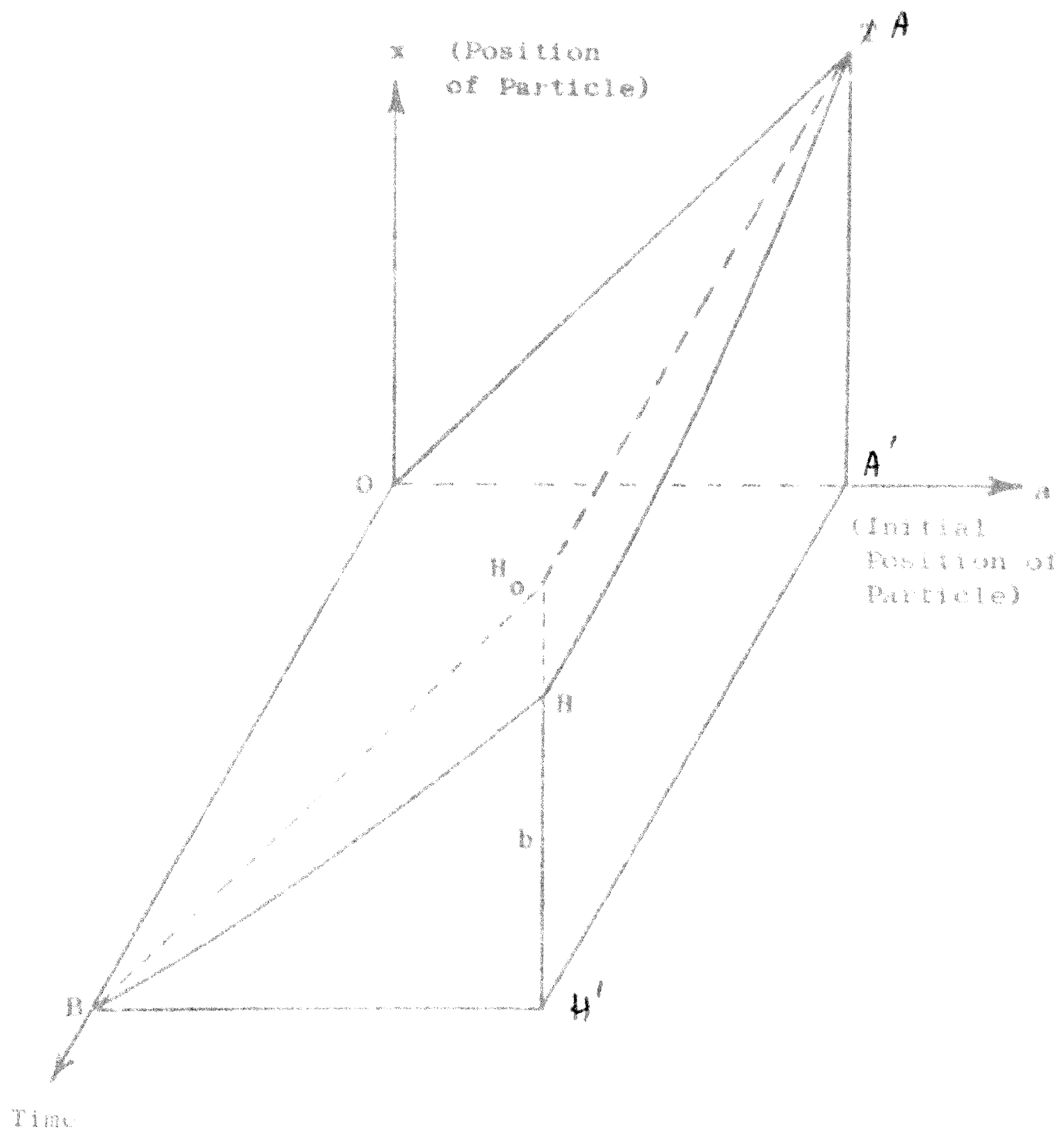


fig.2

Illustration of permeability measurement

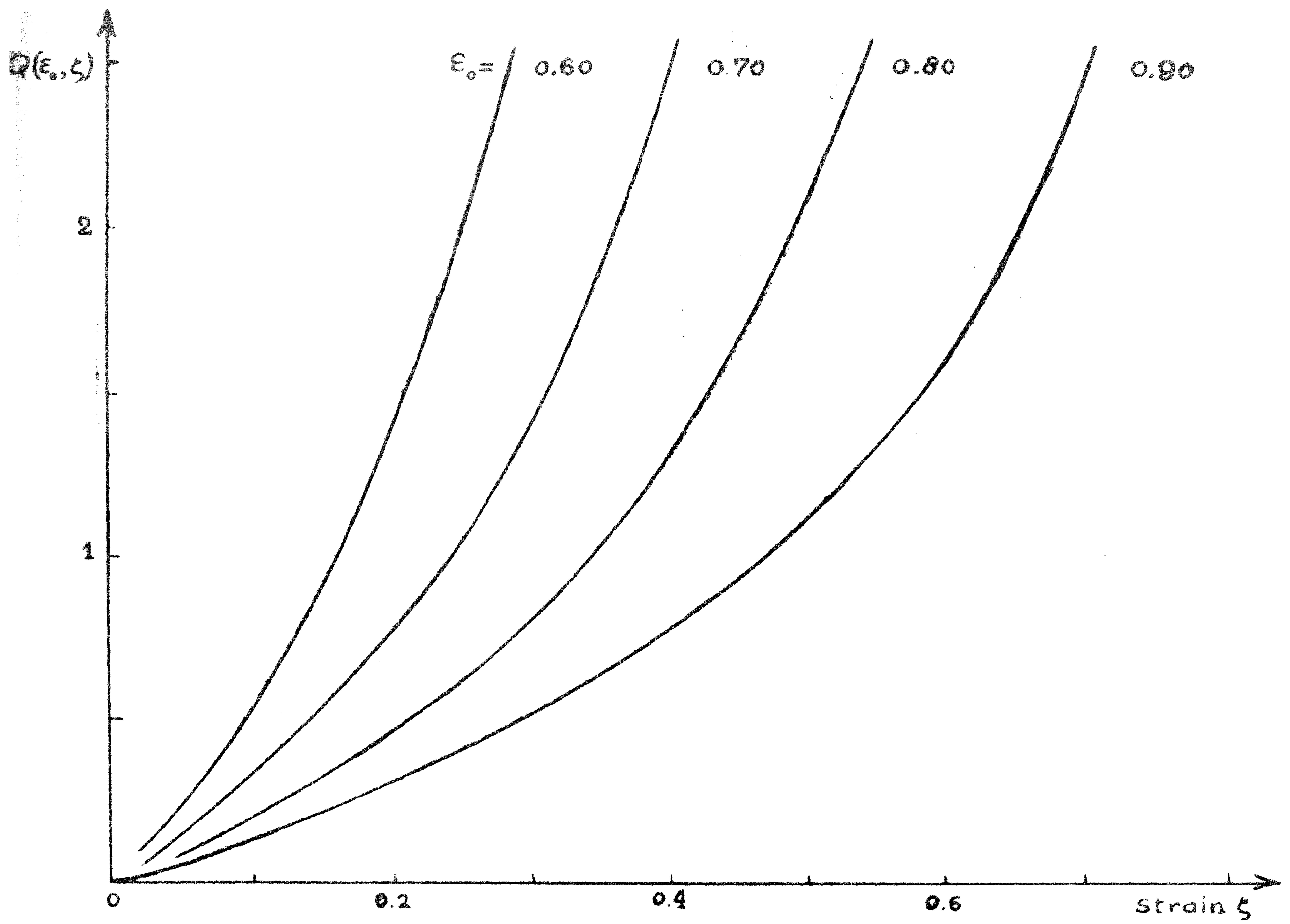


fig.3

Stress-strain relation for solid network. The stress is proportional to \underline{Q} (eq.4.4)

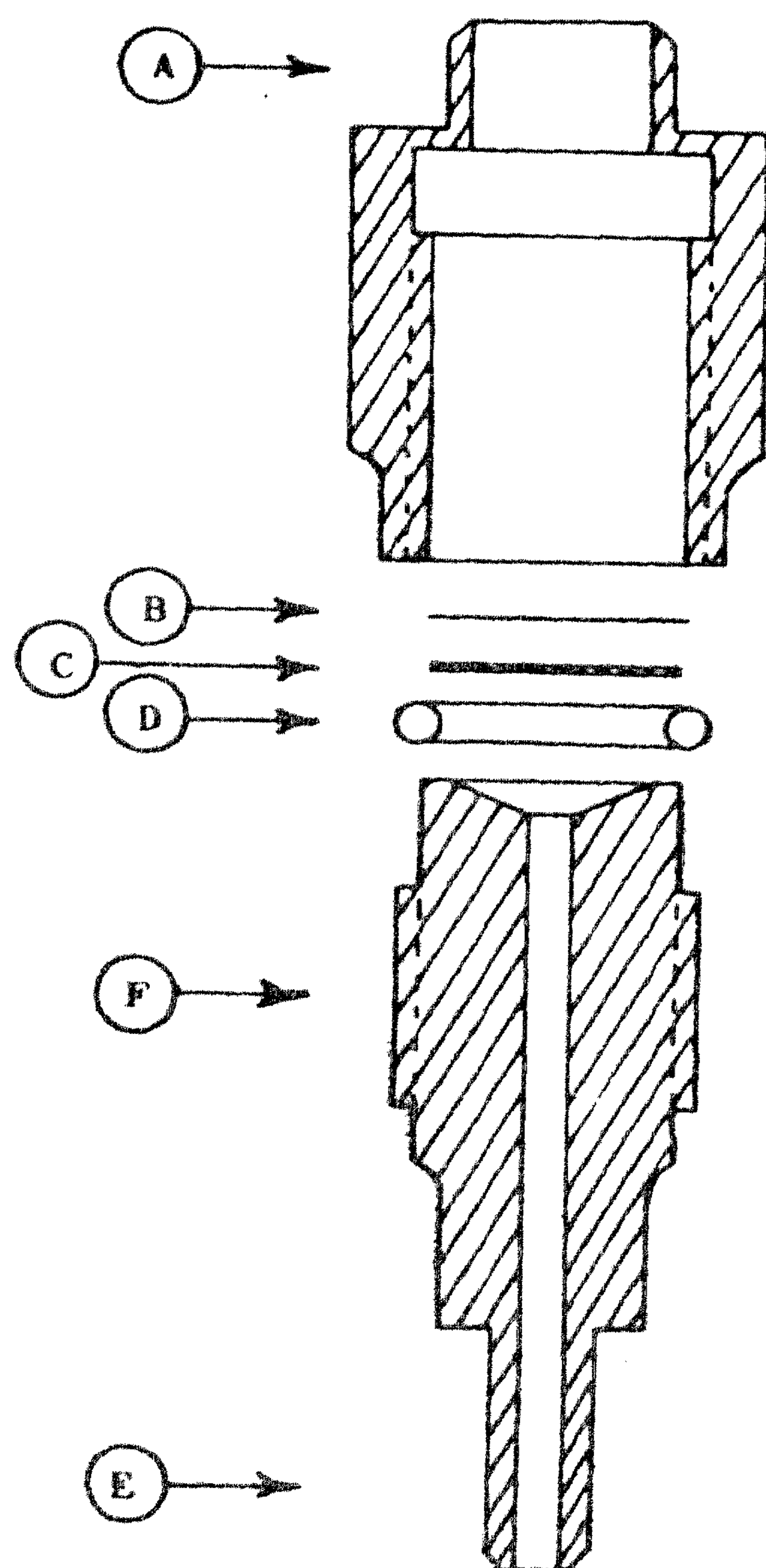


fig.4

Apparatus used for permeability measurements

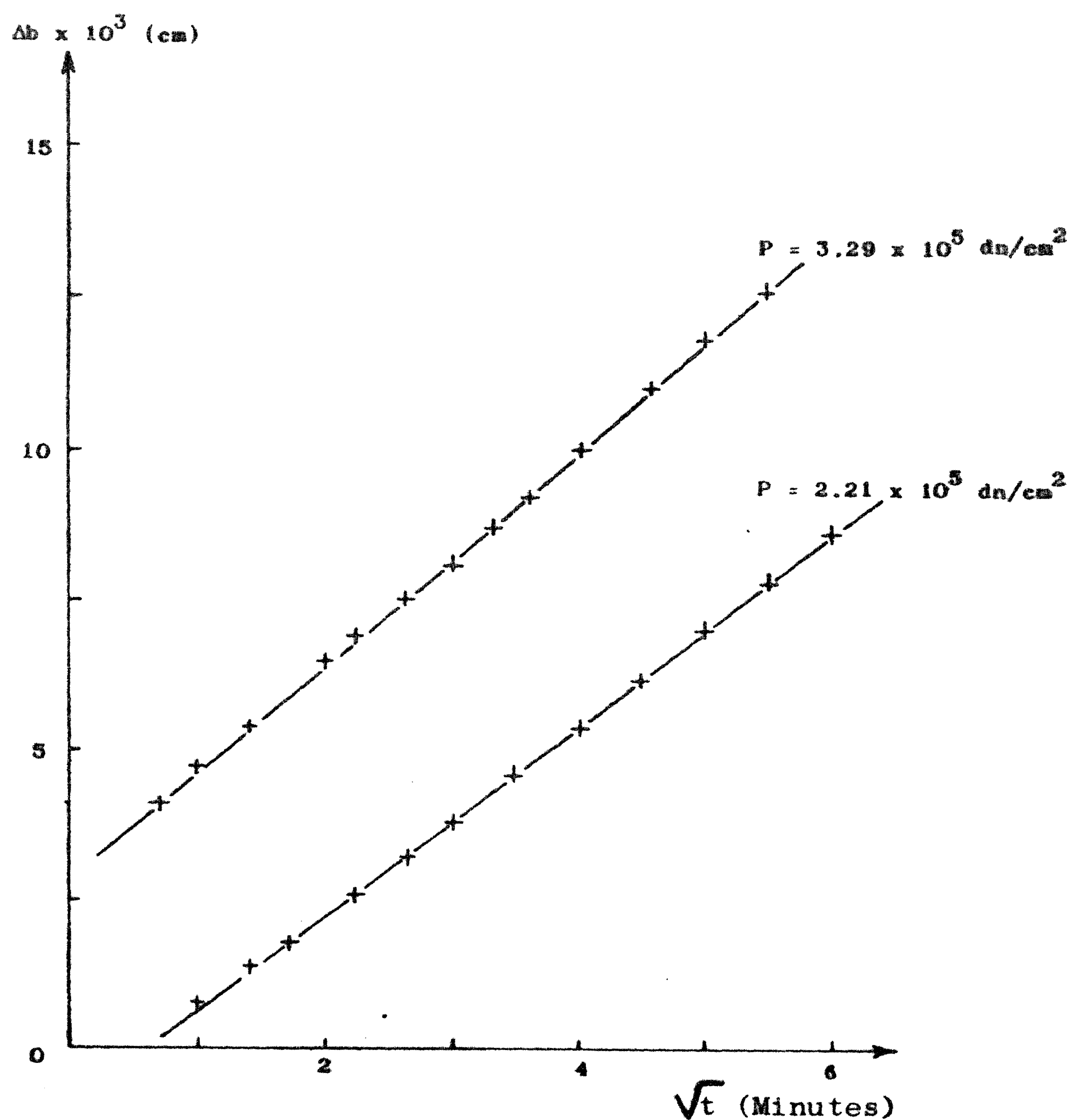


fig.5

Subsidence rate of sample containing 25% tristearate in groundnut oil, crystallized at 30°C

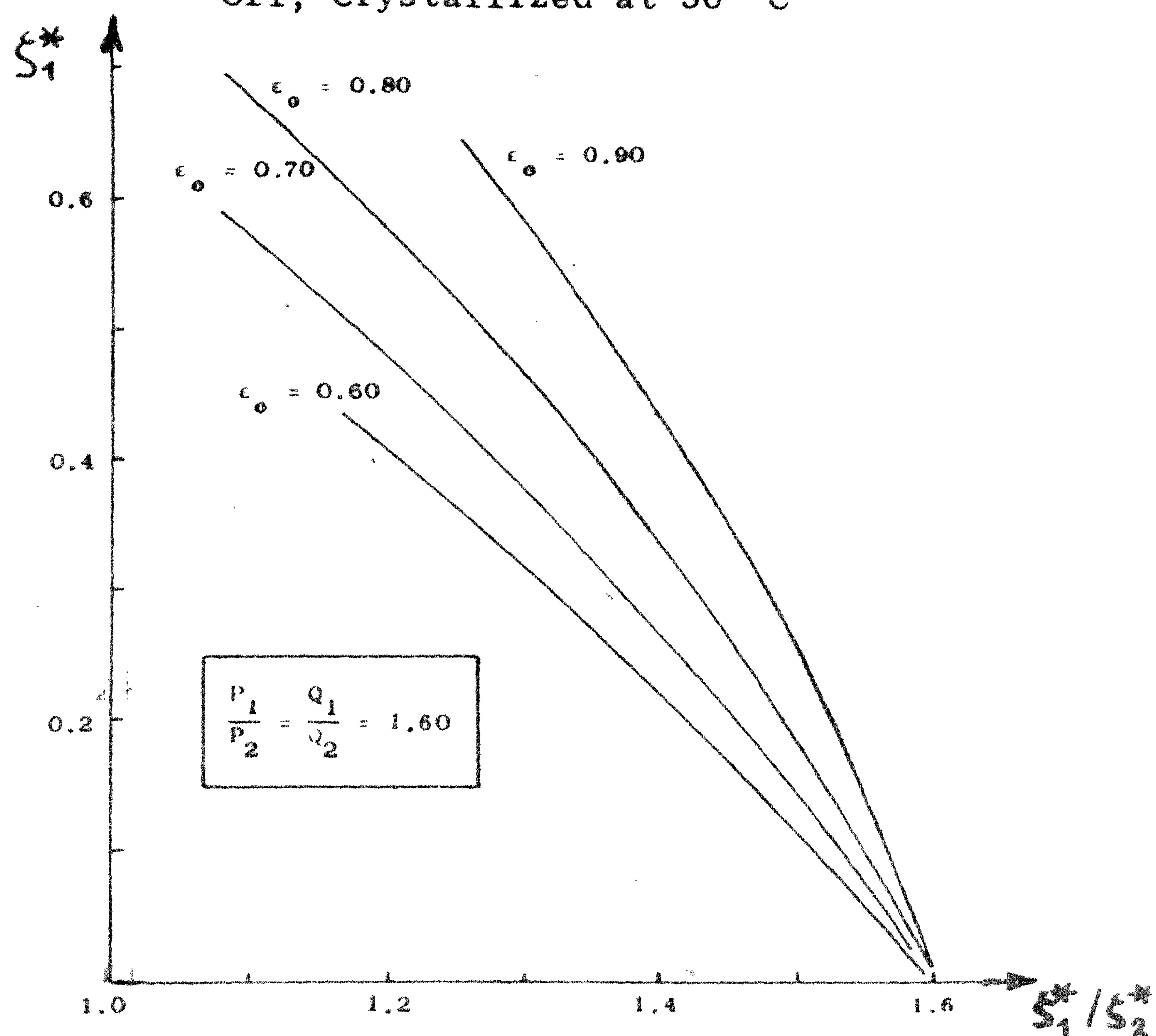


fig.6

Comparison of the strains in the bottom layer of two compression experiments

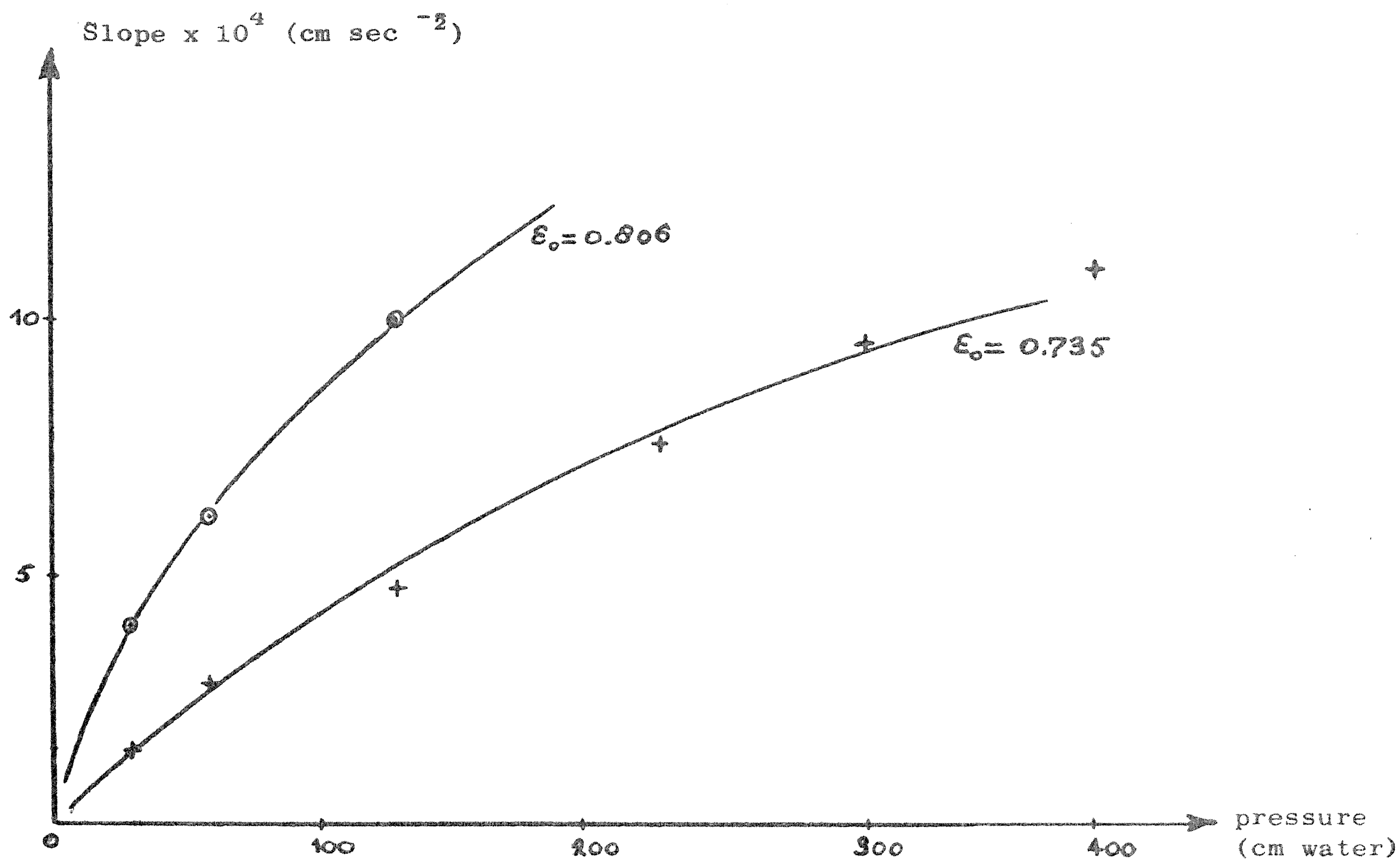


fig.7

Rate of subsidence of samples containing tristearate in paraffin oil. Curves are calculated for $\underline{A}' = 4.77 \times 10^{-6} \text{ cm}^2 \text{ sec}^{-1}$; $\underline{S} = 3.8 \times 10^5 \text{ cm}^{-1}$; $\mu = 0.66$ poise

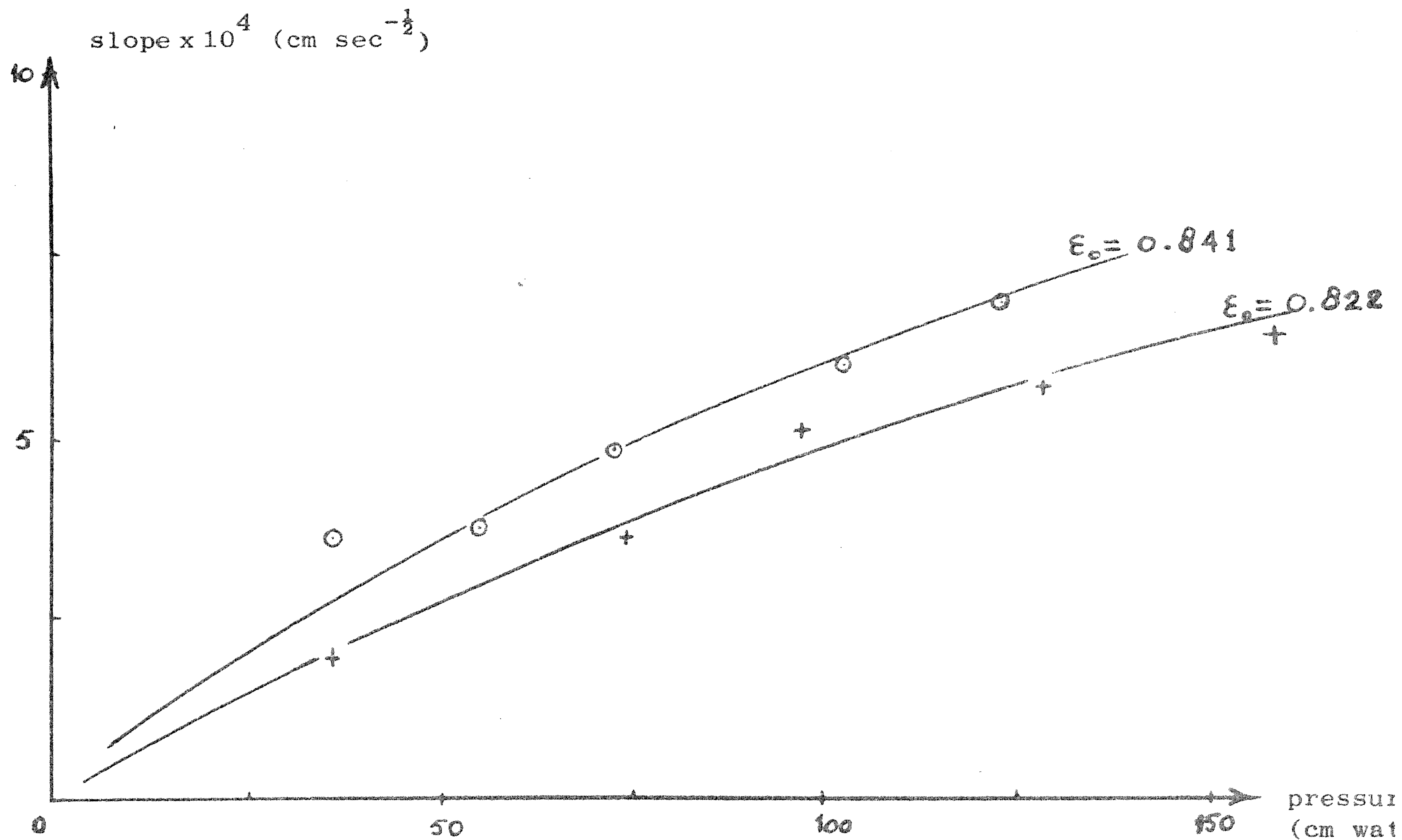
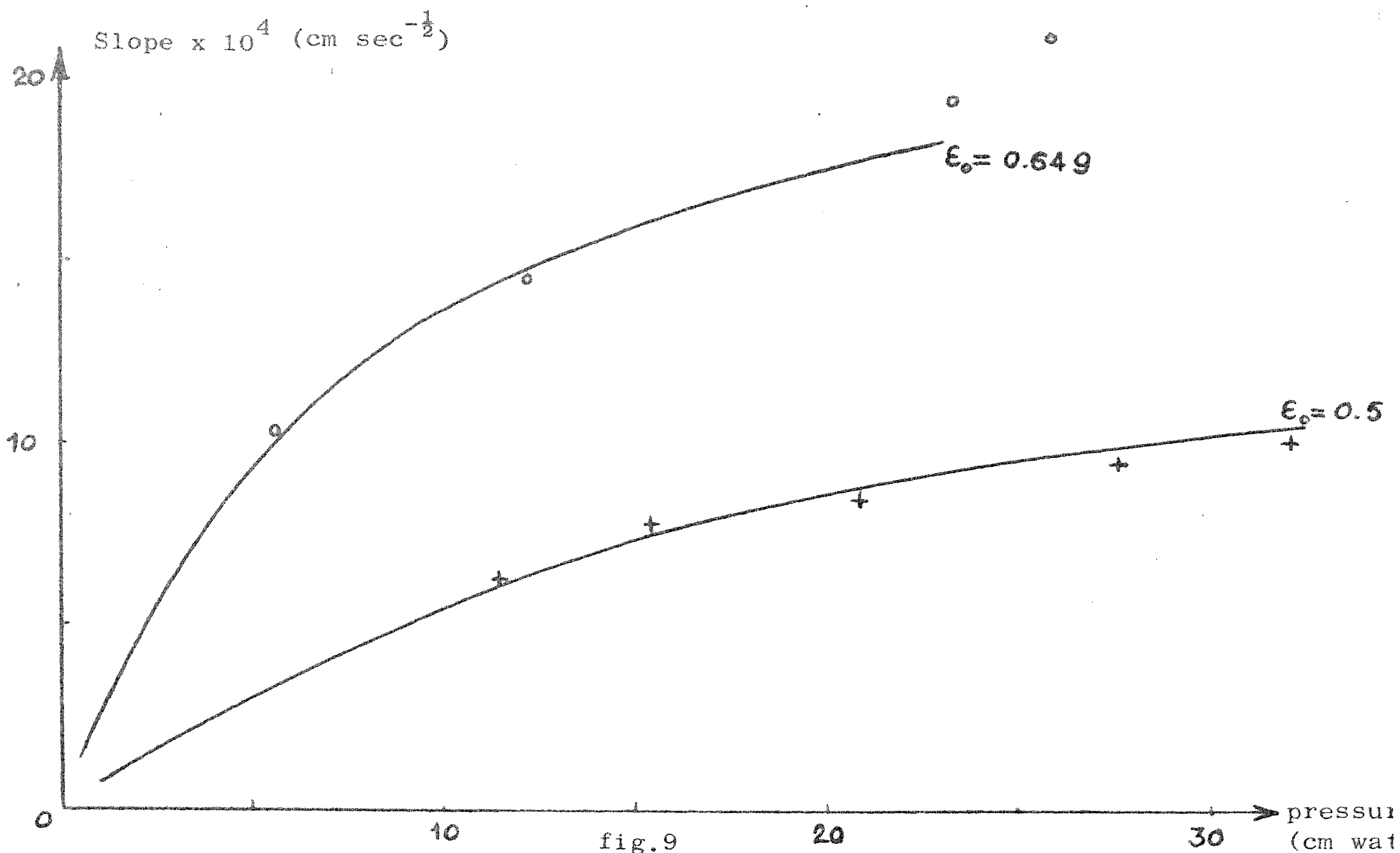
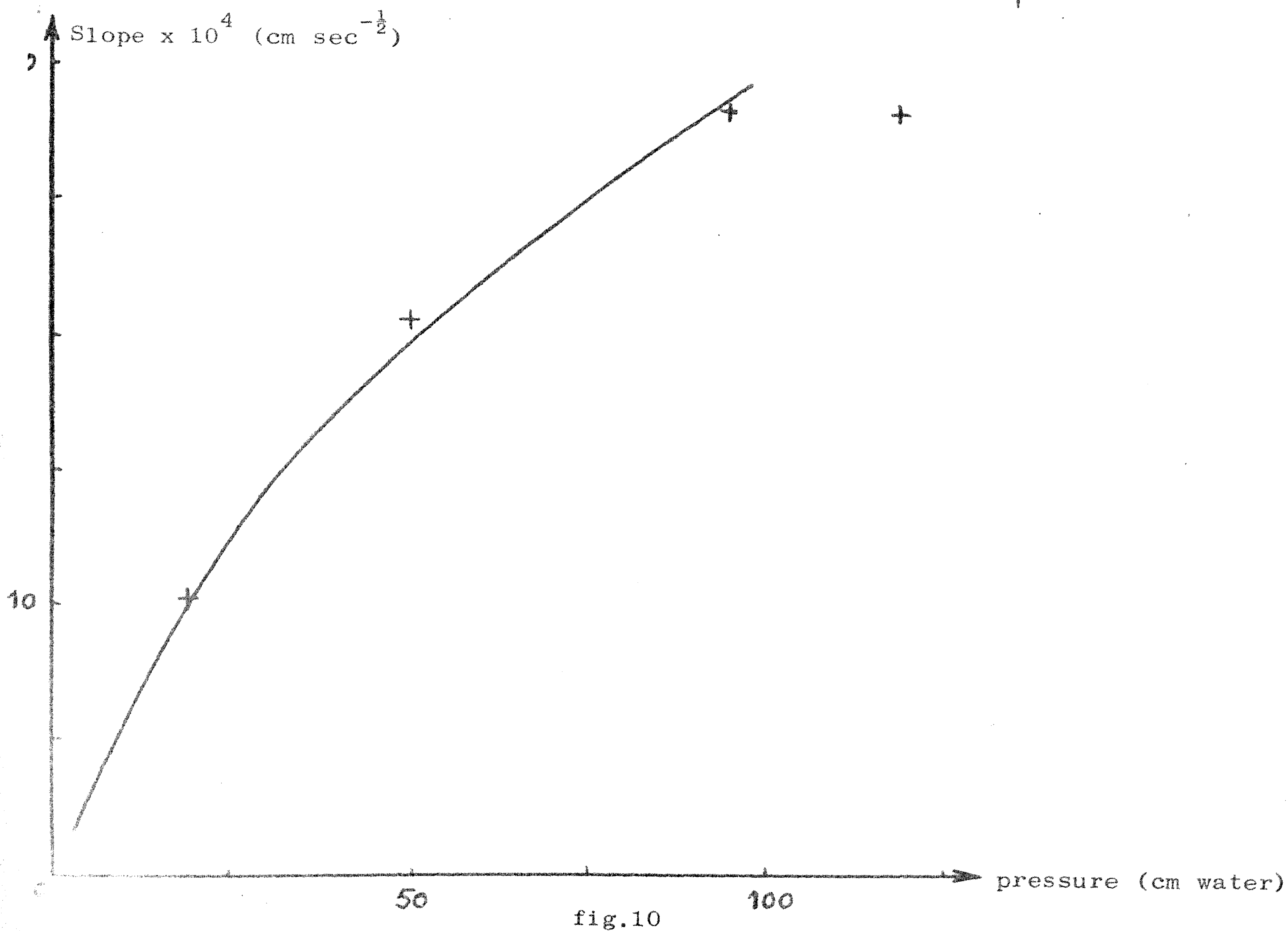


fig.8

Rate of subsidence of samples containing tristearate in groundnut oil. Curves are calculated for $\underline{A}' = 2.36 \times 10^{-6} \text{ cm}^2 \text{ sec}^{-1}$; $\underline{S} = 7.28 \times 10^5 \text{ cm}^{-1}$; $\mu = 0.736$ poise.



Rate of subsidence of samples containing powdered quartz in groundnut oil. Curves are calculated for $A' = 10.9 \times 10^{-6} \text{ cm}^2 \text{ sec}^{-1}$; $S = 2.77 \times 10^4 \text{ cm}^{-1}$; $\mu = 0.78$ poise



Rate of subsidence of samples containing rutile powder in water. Curves are calculated for $A' = 1.04 \times 10^{-5} \text{ cm}^2 \text{ sec}^{-1}$; $S = 2.96 \times 10^6 \text{ cm}^{-1}$; $\epsilon_0 = 0.912$